

# Memory vectors for similarity search in high-dimensional spaces

Ahmet Iscen, Teddy Furon, Vincent Gripon, Michael Rabbat, and Hervé Jégou

**Abstract**—We design an indexing architecture to store and search in a set of high-dimensional vectors. This architecture is composed of several memory vectors, each of which summarizes a fraction of the database by a single representative vector. The membership of the query to the memory vector is tested by a simple correlation with its representative vector. This representative optimizes the membership hypothesis test when the query is a simple perturbation of a stored vector. Compared to exhaustive search, our approach finds the most similar database vectors significantly faster without a noticeable reduction in search quality. Interestingly, the reduction of complexity is provably better in high-dimensional spaces. We empirically demonstrate its practical interest in a large-scale image search scenario. Our evaluation is carried out on standard benchmarks for large-scale image search and uses off-the-shelf state-of-the-art descriptors.

**Index Terms**—High-dimensional indexing, image indexing, image retrieval.

## 1 INTRODUCTION

WE consider the problem of similarity search for large databases. In this context, many papers report how the curse of dimensionality makes indexing ineffective [1], [2]. In the recent paper [2] describing and analyzing the popular FLANN method, it is observed experimentally that even this state-of-the-art method performs poorly on synthetic high-dimensional vectors, and the authors conclude that “random datasets are one of the most difficult problems for nearest neighbor search.”

Some strategies have been proposed to (partly) overcome this problem. For instance, the vector approximation file [1] first relies on exhaustive search with approximate measurements and then computes the exact similarities only for a subset of vectors deemed of interest. The cosine sketch [3] approximates cosine similarity with faster Hamming distance. Set compression tree [4] uses a k-d tree like approach to compress a set of vectors into a compact representation. Other works like spectral hashing [5], Euclidean sketches [6], product quantization [7] and inverted multi-index [8] also rely on compact codes to speed up neighbor search while compressing the data.

This paper proposes a similarity search approach specifically adapted to high-dimensional vectors such as those recently introduced in computer vision to represent images, like the Fisher vector [9]. The proposed indexing architecture consists of memory vectors, each of which is associated with several database vectors. A representative vector is produced for each memory vector and defined such that, by performing a single inner product with a new query, one can quickly and reliably determine whether or not a similar vector is stored.

Our problem is similar to the descriptor pooling problem in computer vision, but at a higher level. Many successful descriptors, such as BOV [10], [11], VLAD [12], FV [9], and EMK [13], encode and aggregate a set of local features into global representations. Although max-pooling and sum-pooling methods have been used traditionally, recent works [14], [15] try to optimize the aggregation step to have a constant similarity between aggregated local features and the global representation. We solve a similar problem at a higher-level; instead of aggregating local features for a global image representation, we aggregate global representations into group representations to perform efficient image search.

We make the following contributions.

- 1) First, we focus on the design of a single memory vector. We formalize the similarity of a query with the vectors of one memory vector as a hypothesis test. We derive the optimal representative vector under some design constraints and show how to compute it in an online manner.
- 2) Second, we propose and analyze a memory array comprising several memory vectors and discuss strategies to store and search vectors with such an architecture.
- 3) Finally, we provide a theoretical analysis with a simple model of the data (uniform distribution over the hypersphere). It reveals the achievable trade-offs and shows that our method is better with higher dimensional data.

We apply this approach to real datasets: descriptors (vectors describing images) extracted with the most recent state-of-the-art algorithm in computer vision [14].

This paper is organized as follows. Section 2 introduces notation, the detection framework considered in the paper, and derives the optimal solution under some assumptions. Section 3 extends the problem to memory vectors, optimizing the design of the indexing system. The experimental section 4 evaluates our approach on standard benchmarks for image search, namely the Oxford building [16], Inria Holidays [17] and UKB [18] datasets. Our results show the potential of our approach for this application.

- A. Iscen, V. Furon and H. Jégou are with Inria.  
E-mail: {ahmet.iscen,teddy.furon,herve.jegou}@inria.fr
- V. Gripon is with Télécom Bretagne.  
E-mail: vincent.gripon@telecom-bretagne.eu
- M. Rabbat is with McGill University.  
E-mail: michael.rabbat@mcgill.ca

## 2 MEMORY VECTORS

Consider a set  $\mathcal{X} = \{\mathbf{x}_1, \dots, \mathbf{x}_n\}$  comprising  $n$  vectors of dimension  $d$ . Our objective is to produce memory vectors such that, given a query vector  $\mathbf{Y}$  regarded as a random variable, we can efficiently perform, loosely speaking, a ‘‘membership’’ test  $[\mathbf{Y} \in \mathcal{X}]$ . The membership holds if  $\mathbf{Y}$  is a quasi-copy of, or similar to, at least one of the vectors stored in the memory vector. For the sake of analysis, this section assumes that all vectors follow a uniform distribution on the  $d$ -dimensional unit hypersphere. The similarity between two vectors  $\mathbf{x}$  and  $\mathbf{y}$  is the inner product  $\langle \mathbf{x} | \mathbf{y} \rangle$ . We model the query as a random vector  $\mathbf{Y}$  distributed according to one of the two laws:

- Hypothesis  $\mathcal{H}_0$ :  $\mathbf{Y}$  is not related to any vector in  $\mathcal{X}$ .  $\mathbf{Y}$  is then uniformly distributed on the unit hypersphere.
- Hypothesis  $\mathcal{H}_1$ :  $\mathbf{Y}$  is related to one vector in  $\mathcal{X}$ , say  $\mathbf{x}_1$  without loss of generality. We write this relationship as  $\mathbf{Y} = \alpha \mathbf{x}_1 + \beta \mathbf{Z}$ , where  $\mathbf{Z}$  is a random vector orthogonal to  $\mathbf{x}_1$  and  $\|\mathbf{Z}\| = 1$ . This means that  $\mathbf{Y}$  is more similar to  $\mathbf{x}_1$  as  $\alpha$  gets closer to 1. We have  $\alpha^2 + \beta^2 = 1$  because  $\|\mathbf{Y}\| = 1$ .

We consider a memory vector satisfying the following design constraints. First, the set of vectors  $\mathcal{X}$  is summarized by a unique  $d$ -dimensional vector  $\mathbf{m}(\mathcal{X}) \in \mathbb{R}^d$ , called the *memory vector* and denoted by  $\mathbf{m}$  when not ambiguous. Then, membership of  $\mathbf{Y}$  to  $\mathcal{X}$  is tested by thresholding the inner product  $\langle \mathbf{m} | \mathbf{Y} \rangle$ .

### 2.1 Sum-memory vector: analysis

A very simple way to define the memory vector is

$$\mathbf{m}(\mathcal{X}) = \sum_{\mathbf{x} \in \mathcal{X}} \mathbf{x}, \quad (1)$$

where we assume that  $\mathcal{X}$  is composed of  $n$  different vectors. Albeit naive, this strategy offers some insights when considering high-dimensional spaces.

Appendix A derives the pdf of the score  $\langle \mathbf{m} | \mathbf{Y} \rangle$  when  $\mathbf{Y}$  is a random vector on the unit hypersphere and  $\mathbf{m}$  is a known vector with fixed norm; this score has expectation 0 and variance  $\|\mathbf{m}\|^2/d$ , and it is asymptotically distributed as  $\mathcal{N}(0, \|\mathbf{m}\|^2/d)$  as  $d \rightarrow \infty$ . This gives an approximate pdf of  $\langle \mathbf{m} | \mathbf{Y} \rangle$  under  $\mathcal{H}_0$ . In contrast, under  $\mathcal{H}_1$ , the inner product equals

$$\langle \mathbf{m} | \mathbf{Y} \rangle = \alpha + \alpha \langle \mathbf{m}(\mathcal{X}') | \mathbf{x}_1 \rangle + \beta \langle \mathbf{m}(\mathcal{X}') | \mathbf{Z} \rangle, \quad (2)$$

with  $\mathcal{X}' = \mathcal{X} - \{\mathbf{x}_1\}$ . This shows two sources of randomness: the interference of  $\mathbf{x}_1$  with the other vectors of  $\mathcal{X}$ , and with the noise vector  $\mathbf{Z}$ . Assuming that  $\mathbf{Y}$  is statistically independent of the vectors in  $\mathcal{X}'$  (this implies that the vectors of  $\mathcal{X}$  are mutually independent), we have

$$\begin{aligned} \mathbb{E}_{\mathbf{Y}}[\langle \mathbf{m} | \mathbf{Y} \rangle | \mathcal{H}_1] &= \alpha, \\ \mathbb{V}[\langle \mathbf{m} | \mathbf{Y} \rangle | \mathcal{H}_1] &= \|\mathbf{m}(\mathcal{X}')\|^2/d. \end{aligned} \quad (3)$$

Assuming that  $\mathcal{X}$  is composed of  $n < d$  statistically independent vectors on the unit hypersphere also gives  $\mathbb{E}_{\mathcal{X}}[\|\mathbf{m}(\mathcal{X})\|^2] = n$  and  $\mathbb{E}_{\mathcal{X}'}[\|\mathbf{m}(\mathcal{X}')\|^2] = n - 1$ . To summarize, for large  $d$ , we have the following distribution:

$$\mathcal{H}_0 : \quad \langle \mathbf{m} | \mathbf{Y} \rangle \sim \mathcal{N}(0, n/d), \quad (4)$$

$$\mathcal{H}_1 : \quad \langle \mathbf{m} | \mathbf{Y} \rangle \sim \mathcal{N}(\alpha, (n-1)/d). \quad (5)$$

Making a hard decision by comparing the inner product to a threshold  $\tau$ , the error probabilities (false positive and false negative rates) are given by

$$\mathbb{P}_{\text{fp}} \approx 1 - \Phi\left(\tau \sqrt{d/n}\right) \quad (6)$$

$$\mathbb{P}_{\text{fn}} \approx \Phi\left((\tau - \alpha) \sqrt{d/(n-1)}\right), \quad (7)$$

where  $\Phi(x) = \frac{1}{\sqrt{2\pi}} \int_{-\infty}^x e^{-t^2/2} dt$ .

The number of elements one can store in a sum-memory vector is linear with the dimension of the space when vectors are drawn uniformly on the unit hypersphere. This construction is therefore useful for high-dimensional vectors only, as opposed to traditional indexing techniques that work best in low-dimensional spaces. Figure 1 depicts Receiver Operating Characteristic (ROC) curves for two ratios  $n/d$  and two values of  $\alpha$ . As expected the test performs better when  $\alpha$  is closer to 1 and when  $n \ll d$ .

If the vectors are pair-wise orthogonal, the dominant source of randomness (the interference between  $\mathbf{x}_1$  and vectors of  $\mathcal{X}'$ ) is cancelled in (2). The variance under  $\mathcal{H}_1$  reduces to  $\beta^2(n-1)/d$ . This prevents any false negatives if  $\beta \rightarrow 0$ . We further exploit this intuition that orthogonality helps in the next section.

### 2.2 Optimization of the hypothesis test per unit

We next consider optimizing the construction of the memory vector when the set  $\mathcal{X}$  consists of a batch of  $n$  vectors known at encoding time. Denote the  $d \times n$  matrix  $\mathbf{X} = [\mathbf{x}_1, \dots, \mathbf{x}_n]$ . We impose that, for all  $i$ ,  $\langle \mathbf{x}_i | \mathbf{m}(\mathcal{X}) \rangle = 1$  exactly and not only in expectation, as assumed above. In other words,  $\mathbf{X}^\top \mathbf{m} = \mathbf{1}_n$  where  $\mathbf{1}_n$  is the length- $n$  vector with all entries equal to 1. Achieving this, when  $\mathbf{Y} \in \mathcal{X}$ , we eliminate the interference with the remaining vectors in  $\mathcal{X}'$  which was previously the dominant source of noise. In other words, under  $\mathcal{H}_1$ , Eq. (2) becomes

$$\langle \mathbf{m} | \mathbf{Y} \rangle = \alpha + \beta \langle \mathbf{m} | \mathbf{Z} \rangle. \quad (8)$$

Under  $\mathcal{H}_0$ , the variance of the score remains  $\|\mathbf{m}\|^2/d$ . Therefore, the norm of the memory vector is the key quantity determining the false positive probability.

We thus seek the representation  $\mathbf{m}$  minimizing the energy  $\|\mathbf{m}\|^2$  subject to the constraint that  $\mathbf{X}^\top \mathbf{m} = \mathbf{1}_n$ . If multiple solutions exist, the minimal norm solution is given by the *Moore-Penrose pseudo-inverse* [19]:

$$\mathbf{m}^* = (\mathbf{X}^\dagger)^\top \mathbf{1}_n. \quad (9)$$

Since  $n < d$ ,  $\mathbf{m}^* = \mathbf{X}(\mathbf{X}^\top \mathbf{X})^{-1} \mathbf{1}_n$ .

If no solution exists,  $\mathbf{m}^*$  is a minimizer of  $\|\mathbf{X}^\top \mathbf{m} - \mathbf{1}_n\|$ . This formulation amounts to treating the task of image search as a linear regression problem [20] with the objective of minimizing

$$\frac{1}{2} \|\mathbf{X}^\top \mathbf{m} - \mathbf{1}_n\|^2 \quad (10)$$

over  $\mathbf{m}$ . Taking the gradient, setting it equal to zero, and solving for  $\mathbf{m}$  gives back  $\mathbf{m}^*$ .

When possible, and for large  $d$ , this new construction leads to the distributions:

$$\mathcal{H}_0 : \quad \langle \mathbf{m}^* | \mathbf{Y} \rangle \sim \mathcal{N}(0, \|\mathbf{m}^*\|^2/d) \quad (11)$$

$$\mathcal{H}_1 : \quad \langle \mathbf{m}^* | \mathbf{Y} \rangle \sim \mathcal{N}(\alpha, \beta^2 \|\mathbf{m}^*\|^2/d). \quad (12)$$

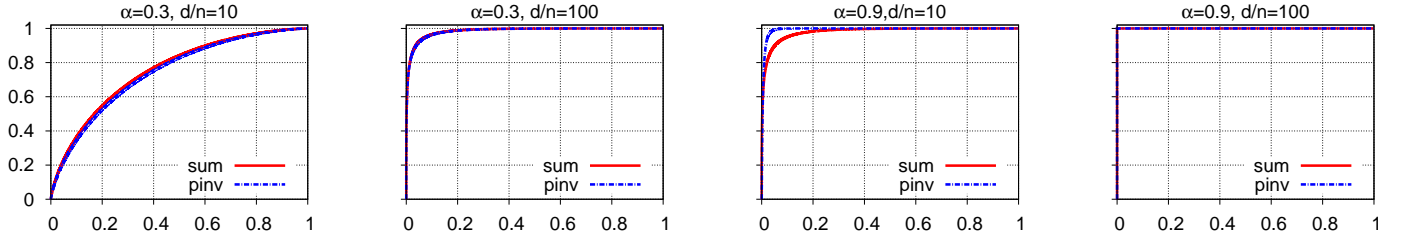


Fig. 1. ROC curves ( $1 - \mathbb{P}_{fn}$  as a function of  $\mathbb{P}_{ip}$ ) for sum and pseudo inverse units using Eq. (6) and (13), evaluated for  $d/n \in \{1000, 10\}$ .

**Algorithm 1** Online optimization of a sum-memory vector. At initialization,  $\mathbf{m} = \mathbf{0}$  and  $\mathcal{R} = \emptyset$ .

At reception of a new vector  $\mathbf{x}$  with unit norm

$$\mathbf{r} \leftarrow \mathbf{x} - \sum_{\mathbf{r}' \in \mathcal{R}} \frac{\langle \mathbf{x} | \mathbf{r}' \rangle}{\langle \mathbf{r}' | \mathbf{r}' \rangle} \mathbf{r}' \quad (\text{classical Gram-Schmidt step})$$

$$\mathcal{R} \leftarrow \mathcal{R} \cup \{\mathbf{r}\}$$

$$\text{If } \langle \mathbf{r} | \mathbf{x} \rangle \neq 0, \text{ then } \mathbf{m} \leftarrow \mathbf{m} + \frac{1 - \langle \mathbf{m} | \mathbf{x} \rangle}{\langle \mathbf{r} | \mathbf{x} \rangle} \mathbf{r}$$

The major improvement comes from the reduction of the variance under  $\mathcal{H}_1$  for small values of  $\beta^2$ . Appendix B shows that, in expectation,  $\|\mathbf{m}^*\|^2$  is larger than the square norm of the naive sum representation from Section 2.1. The reduction of the variance under  $\mathcal{H}_1$  comes at the price of an increase of the variance under  $\mathcal{H}_0$ . However, this increase is small if  $n/d$  remains small. For large  $d$ , we have

$$\mathbb{P}_{ip} \approx 1 - \Phi\left(\tau \sqrt{\frac{d}{n} - 1}\right), \quad (13)$$

$$\mathbb{P}_{fn} \approx \Phi\left(\frac{\tau - \alpha}{\beta} \sqrt{\frac{d}{n} - 1}\right). \quad (14)$$

Note that  $\beta = \sqrt{1 - \alpha^2}$  is a decreasing function of  $\alpha$ . Therefore, if  $\tau < \alpha$ ,  $\mathbb{P}_{fn}$  is a decreasing function of  $\alpha$ . In particular  $\mathbb{P}_{fn} \rightarrow 0$  when  $\alpha \rightarrow 1$  as claimed above. In contrast to the naive sum approach from Section 2.1, for the optimized approach there are no false negatives when the query  $\mathbf{Y}$  is exactly one of the vectors in  $\mathcal{X}$ . This holds for any value of  $\tau < 1$  when  $\alpha = 1$ , so that the false positive rate can be as low as  $1 - \Phi(\sqrt{d/n - 1})$ .

**Remark.** This solution is identical (up to a regularization) to the “generalized max-pooling” method introduced to aggregate local image descriptors [15]. However in our case the aggregation is performed on database side only, as our solution is derived from the hypothesis test associated with a vector-to-set comparison (and not a set-to-set comparison).

### 2.3 Online processing

In Section 2.2, we solved a *batch* linear regression problem. That is, we assumed that we had access to all the vectors stored in the dataset. In practice, the vectors to be stored in the memory vector are not necessarily known in advance. It then becomes meaningful to propose online strategies.

We assume that the number of vectors to store is smaller than the dimensionality of the vectors. Intuitively, when storing a new vector we should (a) not change the test scores of previously stored vectors and (b) ensure that the test score of the newly added vector is one. Algorithm 1 guarantees these properties by construction.

To prove this, we consider a sum-memory vector  $\mathbf{m}$  obtained from a set of vectors  $\mathcal{X}$  using this algorithm. Denote by  $\mathbf{x}' \in \mathcal{X}$  a previously stored vector and  $\mathbf{x}$  a new vector that we add to the memory vector. Algorithm 1 keeps a set  $\mathcal{R}$  of the residuals of vectors already stored. The Gram-Schmidt step guarantees that  $\mathbf{x}'$  is in the span of  $\mathcal{R}$ , since  $\text{span}(\mathcal{X}) = \text{span}(\mathcal{R})$ . Thus by construction we have  $\langle \mathbf{x}' | \mathbf{r} \rangle = 0$ . It follows that the test score of  $\mathbf{x}'$  is

$$\langle \mathbf{x}' | \mathbf{m} \rangle + \frac{1 - \langle \mathbf{m} | \mathbf{x} \rangle}{\langle \mathbf{r} | \mathbf{x} \rangle} \langle \mathbf{r} | \mathbf{x}' \rangle = \langle \mathbf{x}' | \mathbf{m} \rangle, \quad (15)$$

which shows that the test score of a vector previously stored in the memory is not affected when adding a new vector. The second property (b) is verified if we assume that the new vector  $\mathbf{x}$  is *not* in the span of  $\mathcal{X}$ , which is satisfied almost surely if  $d > n$ . In this case, the obtained residual vector  $\mathbf{r}$  is nonzero, and we have

$$\langle \mathbf{m} | \mathbf{x} \rangle + \frac{1 - \langle \mathbf{m} | \mathbf{x} \rangle}{\langle \mathbf{r} | \mathbf{x} \rangle} \langle \mathbf{r} | \mathbf{x} \rangle = 1, \quad (16)$$

which proves the second property (b). By induction, this also shows that the memory vector  $\mathbf{m}$  produced by Algorithm 1 satisfies  $\mathbf{X}^\top \mathbf{m} = \mathbf{1}_n$ . Among the solutions satisfying this linear equation, the one from (9) obtained with the pseudo-inverse is the only one such that  $\mathbf{m} \in \text{span}(\mathcal{X})$ . Since the memory vector produced by the online algorithm also satisfies this property by construction, we conclude that the constructions of  $\mathbf{m}$  with (9) and Algorithm 1 are equivalent.

Adding several times the same vector does not change the value of  $\mathbf{m}$ , as  $\mathbf{r}$  is  $\mathbf{0}_d$  in such case. The resulting memory vector produced by the online algorithm does not depend on the order in which the data vectors are processed. The complexity of Algorithm 1 is  $\mathcal{O}(dn)$  operations. The global complexity after storing all elements of  $\mathcal{X}$  is therefore  $\mathcal{O}(dn^2)$ .

## 3 MEMORY VECTORS AND APPLICATION

From now on, we consider an application scenario where we need to store a large number  $N$  of vectors and perform similarity search. One memory vector is not sufficient to achieve a reliable test. We therefore consider an architecture that consists of several memory vectors. The search strategy is as follows. A given query vector is compared with all the memory vectors. Then we compare the query with the vectors stored in the memory vectors associated with the high responses, i.e., those likely to contain a vector close to the query. The main question that we consider in this section is: how many vectors per memory vector should we store to achieve the best complexity/accuracy trade-off?

**Analysis.** We suppose that the  $N$  vectors in the database are grouped into  $M$  units of  $n$  vectors:  $N = nM$ . We aim at finding the best  $n$ . When the query is related to the database (i.e., under

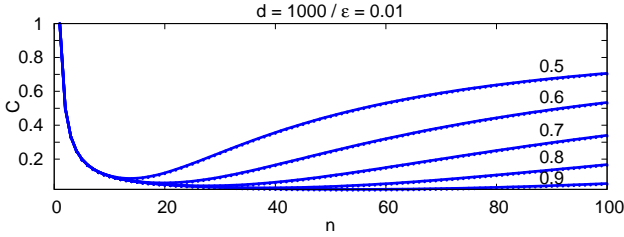


Fig. 2. Ratio of the global cost by the cost of the exhaustive search  $C_{\mathcal{H}_0}/N$  as a function of  $n$ . Setup:  $d = 1000$ ,  $\epsilon = 10^{-2}$ . The different curves correspond to values of  $\alpha_0 = [0.5, 0.9]$ .

$\mathcal{H}_1$ ), we make the following assumption:  $\alpha_0 < \alpha < 1$ , and we fix the following requirement:  $\mathbb{P}_{\text{fn}} < \epsilon < 1/2$ . Since  $\mathbb{P}_{\text{fn}}$  is an increasing function of  $\alpha$ , we need to ensure that  $\mathbb{P}_{\text{fn}}(\alpha_0) = \epsilon$ . This gives us the following threshold  $\tau$ :

$$\tau = \alpha_0 + \sqrt{\frac{1 - \alpha_0^2}{d/n - 1}} \Phi^{-1}(\epsilon). \quad (17)$$

Note that  $\Phi^{-1}(\epsilon) < 0$  because  $\epsilon < 1/2$  so that  $\tau < \alpha$ . Putting back this expression in (13), we obtain a probability of false alarm which only depends on  $n$ , denoted by  $\mathbb{P}_{\text{fp}}(n)$ . This is indeed an increasing function. Now, we decide to minimize the total computational cost  $C_{\mathcal{H}_0}$  when the query is not related. We need to compute one inner product  $\langle \mathbf{m}_j | \mathbf{y} \rangle$  per unit, and then to compute  $n$  inner products  $\langle \mathbf{x}_i | \mathbf{y} \rangle$  for the units giving a positive detection. In expectation, there are  $M \cdot \mathbb{P}_{\text{fp}}(n)$  such units, and so

$$C_{\mathcal{H}_0} = M + M \cdot \mathbb{P}_{\text{fp}}(n) \cdot n = N(n^{-1} + \mathbb{P}_{\text{fp}}(n)). \quad (18)$$

The total cost is the sum of a decreasing function ( $n^{-1}$ ) and an increasing function ( $\mathbb{P}_{\text{fp}}(n)$ ), which implies that there is a tradeoff between having a few big units ( $n$  large) and many small units ( $n$  small). Fig. 2 illustrates this tradeoff for different values of  $\alpha_0$ . It is not possible to find a closed form expression for the cost minimizer  $n^*$ . When  $\alpha_0$  is close to 1, the threshold is set to a high value, producing reliable tests, and we can pack many vectors into each unit;  $n^*$  is large allowing a huge reduction in complexity. Even when  $\alpha_0$  is as small as 0.5,  $n^*$  is small but the improvement remains significant; the proposed approach has a complexity that is less than one tenth of that of searching through all database vectors (equivalent to  $n = 1$ ). This is confirmed by our experiments on real data presented in Section 4. In order to increase the efficiency, we introduce an additional  $\mathcal{O}(Md) = \mathcal{O}(dN/n)$  memory overhead using memory vectors.

## 4 EXPERIMENTS

This section shows that memory vectors perform extremely well with real data. We consider the two constructions for memory vectors introduced in Section 2: naive *sum* and the version optimized using the pseudo-inverse (referred to as *pinv* from now on).

### 4.1 Evaluation Protocol

**Datasets.** We use the Inria Holidays [17], Oxford5k [16], and UKB [18] image datasets in our experiments. Additionally, we conduct a large scale experiment by adding images from the Flickr1M [16] dataset to the Holidays dataset.

**Descriptors.** We use the state-of-the-art triangular embedding descriptor [14], denoted by  $\phi_\Delta$ . We use the off-the-shelf reference

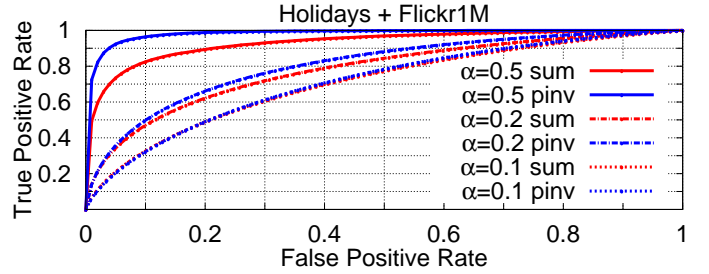


Fig. 3. Cosine similarity experiments for Holidays+Flickr1M using  $\phi_\Delta$  features with  $d = 1920$ .

implementation provided by the authors, which can be found online.<sup>1</sup> Each image is represented by a feature vector. The only difference is that we do not apply the “powerlaw normalization” to better illustrate the benefit of the *pinv* technique for the memory vector construction compared to the *sum* (when applying the powerlaw normalization, both designs perform equally well since the vectors are nearly orthogonal). Ultimately, we have  $d = 8096$  (or  $d = 1920$ ) dimensional feature vectors for each image, obtained by using a vocabulary of size 64 (resp. 16).

We also experiment using deep learning features provided by Babenko *et al.* [21]. As explained in their paper, the performance for the UKB dataset drops with adapted features trained on the Landmarks dataset. Therefore, we use the original neural codes trained on ILSVRC for the UKB dataset, and the adapted features ( $d = 4096$  dimensions) for Holidays and Oxford5k.

**Performance.** Unless stated otherwise, our experimental analysis follows the standard image retrieval protocol where each image is represented by a feature vector and the ground truth is based on the visual similarity. The goal is to return visually similar images for a given query image. The similarity of two images is measured by the cosine of their descriptor vectors, and the images are ordered accordingly. We adopt the performance measure defined for each benchmark (mAP or 4-recall@4, the higher the better).

**Complexity.** Following Section 3, we measure the similarity between the query and memory vectors, and re-rank all the images in memory vectors that have similarity above a threshold  $\tau$ . We characterize the complexity of the search per database vector by:

$$C_{\mathcal{H}_1}(\tau) = M + n \cdot M_p(\tau), \quad (19)$$

where  $M_p(\tau)$  is the number of positive memory vectors per query that are above the threshold  $\tau$ . Fig. 4 shows that  $M = N/10$  memory vectors provide the best trade-off for  $\phi_\Delta$  descriptors on the Holidays dataset. The same behaviour also applies for the other datasets. We measure the complexity ratio  $C_{\mathcal{H}_1}(\tau)/N$  and the retrieval performance for different values of the threshold  $\tau$ . For large  $\tau$ , no memory vector gives a positive output, resulting in  $C_{\mathcal{H}_1}(\tau)/N = M$  and no candidate is returned. As  $\tau$  decreases, more memory vectors trigger reranking.

### 4.2 Comparison of *pinv* vs *sum*

**Cosine similarity-** based ground truth is one way to measure the performance since it is directly related with the model we considered previously. For each query vector we deem a database vector as relevant if their cosine similarity is greater than  $\alpha_0$ , regardless

1. <http://www.tinyurl.com/democratic-kernel>

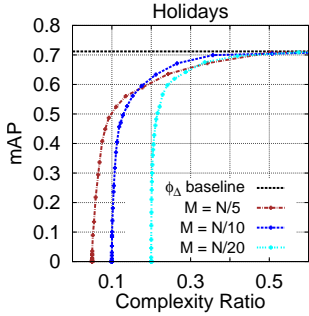


Fig. 4. Image retrieval performance using different number of memory units ( $M$ ) for *pinv* construction.  $M = N/10$  gives the best trade-off for  $\phi_{\Delta}$  features.

of their visual information. To have enough ground-truth vectors, we perform this experiment on the Holidays+Flickr1M dataset using various  $\alpha_0$  values, and report the ROC curve in Fig. 3. The performance gain of *pinv* over *sum* for memory vector design is significant when  $\alpha_0$  is higher, but it decreases with  $\alpha_0$ .

**Visual similarity**-based ground truth tells a different story: Fig. 5 shows a very slight difference between *pinv* and *sum*. This is probably due the big range of vector similarity values between images deemed as visually similar.

We now propose another assignment strategy: we group similar vectors in the same memory vector. For this purpose, we adopt the spherical  $k$ -means clustering [22] with  $k = M$  instead of random assignment. For the *pinv* aggregation case, we modify the update stage of spherical  $k$ -means to represent clusters using *pinv* instead of *sum*. Matlab code for this algorithm is shown on Algorithm 2. However, when we use a such an assignment method, the number of vectors per memory vector is not evenly distributed. The independence assumption made in the previous sections no longer holds. To have comparable similarity scores for unevenly distributed memory vectors, we normalize the similarity score for each memory vector to a probability value between 0 and 1 by dividing it by the squared-norm of the memory vector. This mapping is done every time we have a dot product between a memory vector and a query (see Algorithm 2). Fig. 5 shows that this strategy brings a significant improvement compared to the random assignment. Unless otherwise mentioned, in the remainder of the paper we adopt spherical  $k$ -means for the assignment of vectors to memory vectors. Note that it may not be computationally tractable to use this assignment method for very large databases, such as the Holidays+Flickr1M dataset, and Section 4.3 discusses another assignment strategy for large datasets.

### 4.3 Versatility

This subsection demonstrates that memory vectors indexing is compliant with usual mechanisms in the image search literature.

**The dimensionality** of the descriptor linearly impacts the efficiency of any system. Dimensionality reduction with PCA is one way to improve this point. Our method is compatible with dimensionality reduction as shown in Fig. 6, where we reduce the vectors to  $d' = 1024$  components. It achieves performance comparable to the baseline with lower computational complexity.

We also apply our method to features learned with deep learning ( $d = 4096$ ). Fig. 7 shows that the reduction in complexity also applies when using high performance deep learning features, although there is no significant difference between *pinv* and *sum*. Note that, optimal setting for the Oxford5k dataset using these features is with  $M = N/5$ . Although these features are not centered, and do not follow our assumptions, we show that our approach still obtains efficient performance.

### Algorithm 2 : Memory vector $k$ -means Matlab code.

A modified version of spherical  $k$ -means algorithm, where the update stage is either *pinv* or *sum* depending on memory vector aggregation method. We also treat cluster centers as memory vectors, and instead of normalizing them to a unit norm, we normalize their similarity scores by dividing them by squared-norm of each cluster vector using *sNormalize* function.

#### Inputs

- $X$ : Vectors to be clustered
- $k$ : Number of clusters
- mode: Update mode

#### Outputs

- $C$ : Cluster centers
- $idx$ : Cluster assignments for each vector

```
function [C, idx] = mvectorKmeans(X, k)
niter = 20;
n = size(X, 2);
% Initialization with random vectors
C = X(:, ids);
% Update function. Change it to sum depending on the
% memory vector aggregation method.
updatefunc = @(X,g) pinv(X(:,g)') ...
    *ones(numel(g),1);
for i = 1:niter
    [~,idx] = max(sNormalize(X,M));
    % Identify how to group vectors into clusters
    G = accumarray(idx',1:n,[k 1],@(x){x});
    % Reassign empty clusters
    C(:,cellfun('isempty',G)) = X(:, ...
        randperm(n, sum(cellfun('isempty',G))));
    % Iterate and update over non-empty clusters
    for j=find(~cellfun('isempty',G))'
        C(:,j) = updatefunc(X,G{j});
    end
end
function sM_norm = sNormalize(X,M)
n = size(X, 2);
mnorm = repmat(sqrt(sum(M.^2,1)),1,n);
snorm = ((M' * X)./mnorm);
sM_norm = normcdf(snorm);
end
```

**Compact Codes** are another way to increase efficiency. We reduce the dimensionality of the descriptor vectors to  $d' = 1024$  and binarize them by taking the *sign* of each component, in the spirit of cosine sketches [3]. In the asymmetric case [23], [24], only memory vectors and dataset vectors are binarized, whereas in the symmetric case query vectors are also binarized.

Figures 8 and 9 show the performance when using compact binary codes. For the symmetric case, the *sum* method seems to perform slightly better than *pinv* on the Holidays and Oxford5k datasets. In the asymmetric case, both methods perform similarly. In all cases, we achieve convergence to the baseline with a complexity ratio well below 1. Implementation efficiency is further improved in the symmetric case by using the Hamming distance calculation instead of dot product.

**Large scale experiments.** We conduct large scale experiments on Holidays+Flickr1M, this time using image similarity as a performance measure. When using random assignment of images to groups, the performance is close to the baseline while performing roughly three times fewer vector operations than exhaustive search; see Fig. 10.

**Batch assignment.** We further improve the performance by performing memory unit assignments using *batch spherical k*-

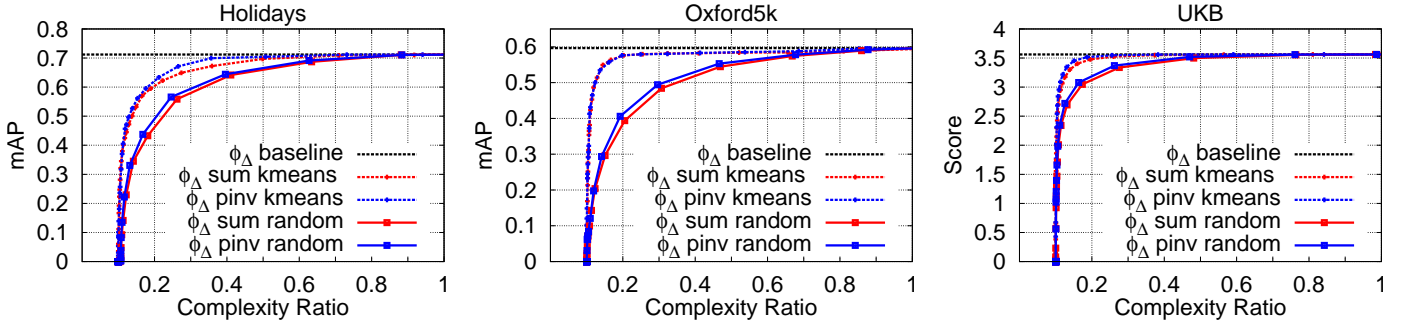


Fig. 5. Image retrieval performance using different assignment methods and visual similarity. K-means (Alg. 2) brings significant improvement.

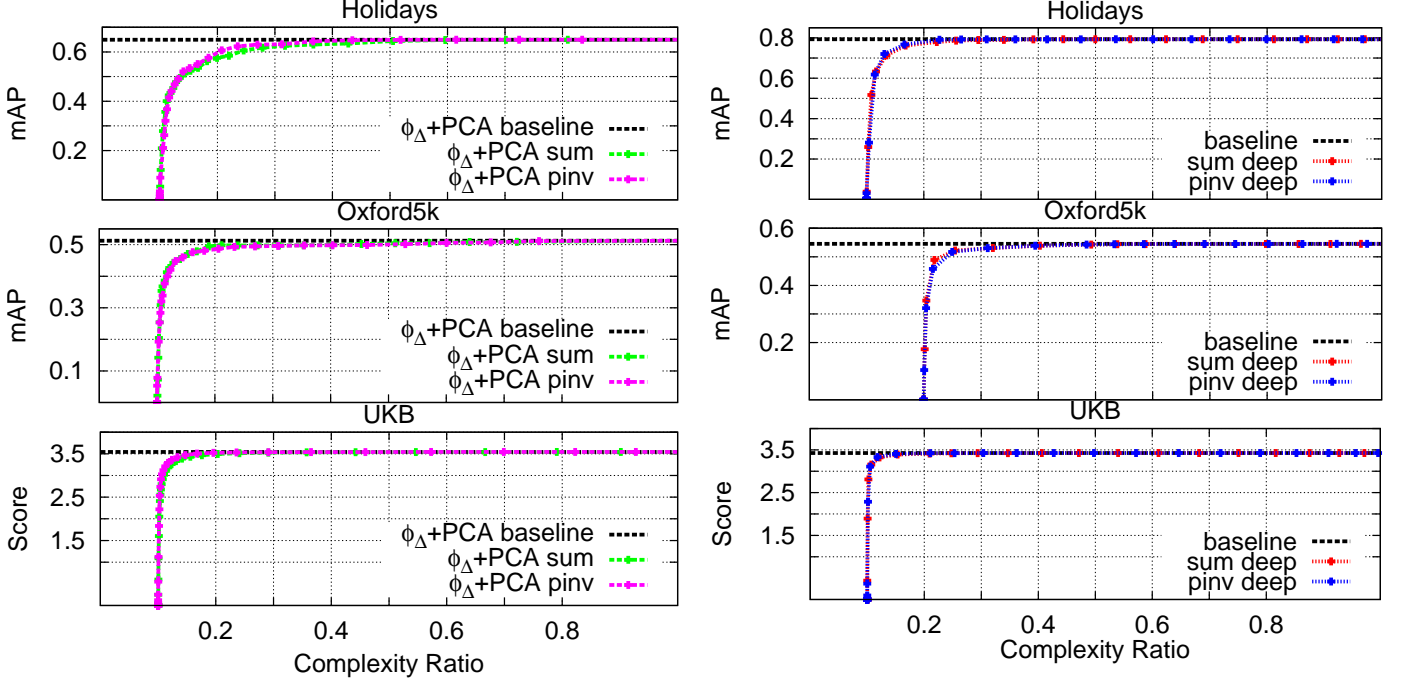


Fig. 6. The performance of memory vectors after PCA dimensionality reduction with  $d' = 1024$ .

Fig. 7. Image retrieval performance with deep learning features ( $d = 4096$ ), as trained by Babenko *et al.* [21]. Features for Holidays and Oxford5K are retrained on the Landmarks dataset, whereas the ones for UKB are trained on ILSVRC.

*means*. This is the same as the regular spherical k-means approach discussed in previous sections, except we do not cluster the whole dataset at once, as this would not be compatible with large collections. Instead, we randomly divide the dataset into batches of same size, and run the clustering algorithm separately for each batch. Fig 11 shows that this strategy improves the performance while keeping the batch size compatible and reducing the complexity of the clustering algorithm.

#### 4.4 Complexity Gain

**Comparison with FLANN [2].** FLANN algorithm on the Holidays+Flickr1M dataset reveals that the convergence to the baseline is achieved with a speed up of 1.25, which translates to a complexity ratio of around 0.8. We can achieve similar performance with a complexity ratio of only 0.3. This confirms that FLANN is not effective for high-dimensional vectors.

**Execution time.** We have shown that we get close to baseline performance while executing significantly fewer operations. We now measure the difference in execution time under a simple setup:

$d = 1024$  and  $N = 1M$  dataset vectors. An average dot product calculation between the query and dataset is  $0.2728s$ . With  $N/10$  memory vectors and  $nM_p \approx 100k$  vectors in positive memory vectors, the execution time decreases to  $0.0544s$ . We improve the efficiency even further by using memory vectors with symmetric compact codes and Hamming Distance computation: the execution time becomes  $0.0026s$ . Our method can be parallelized for even more improvement.

## 5 CONCLUSION

We have presented and analyzed two strategies for designing memory vectors enabling efficient membership tests for real-valued vectors. The first conclusion we draw is that a simple strategy based on sum-aggregation achieves remarkably good results for high-dimensional vectors. Yet it is possible to go beyond this simple strategy by optimizing the hypothesis test under a few assumptions. The resulting approach turns out to be a weighted summation of the stored vectors that can be implemented in an online manner. Interestingly, our approach gives a solution

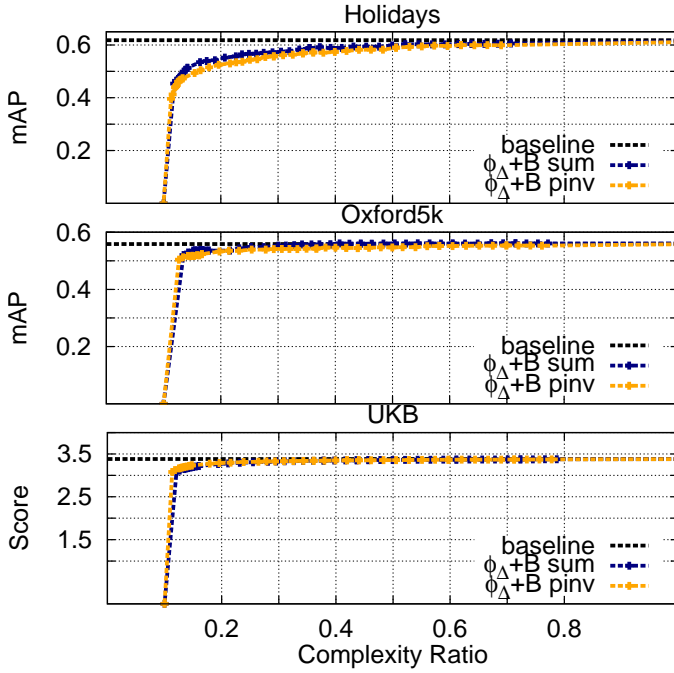


Fig. 8. Experiments with binary codes after PCA reduction to  $d' = 1024$ . The quantization is symmetric: real query vectors are binarized and then compared to binary memory vectors.

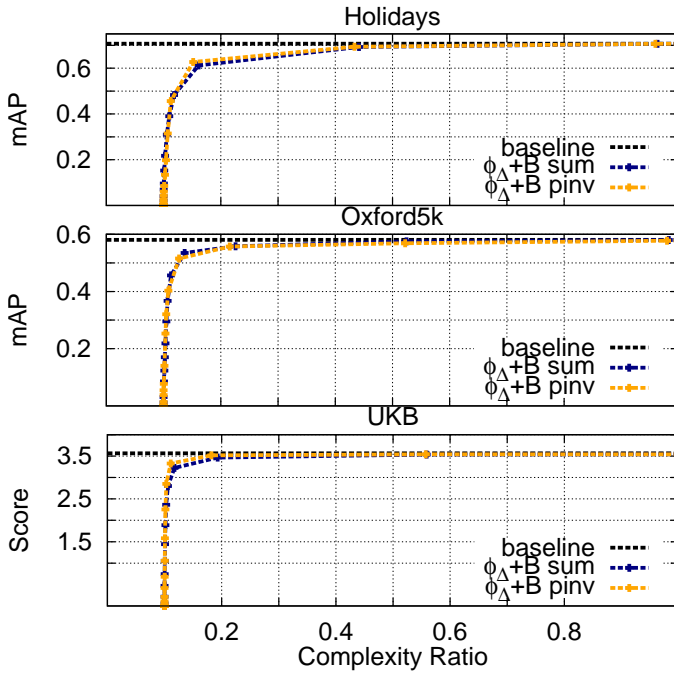


Fig. 9. Experiments with binary codes after PCA reduction to  $d' = 1024$ . The quantization is asymmetric: real query vectors are compared to binary memory vectors.

similar to a method recently introduced to construct image descriptors [15]. We then propose an indexing structure consisting of several memory vectors and determine how to adjust the key parameter to achieve the best possible complexity/accuracy trade-off. Our theoretical analysis is validated by experiments done on standard benchmarks for image retrieval, with datasets comprising up to 1 million images.

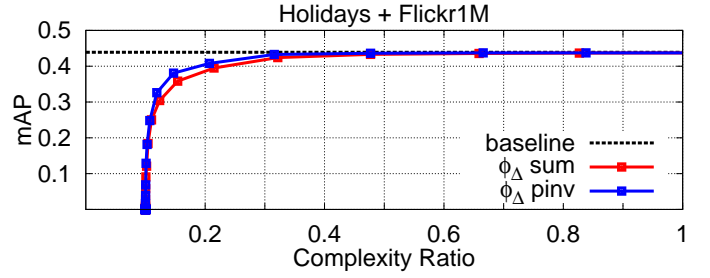


Fig. 10. Image retrieval experiments for Holidays+Flickr1M.  $\phi_\Delta$  with  $d = 1920$ , random assignment for this experiment.

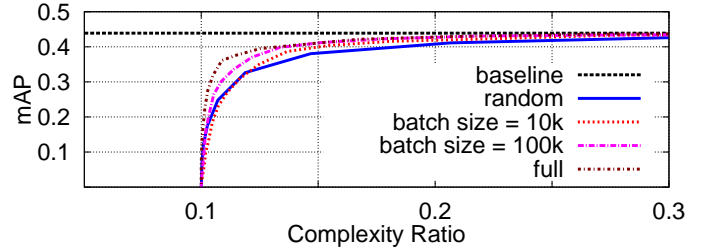


Fig. 11. Comparison of random to batch spherical k-means assignment using different batch sizes in a large-scale setup. Note that the *random* assignment corresponds to batch size of 10, and *full* corresponds to a batch size of 1001491. We run each experiment multiple times.

## APPENDIX A DISTRIBUTION OF A SCALAR PRODUCT

Let  $\mathbf{Y}$  be a random vector uniformly distributed on the unit hypersphere in  $\mathbb{R}^d$  ( $\|\mathbf{Y}\| = 1$ ), and  $\mathbf{m}$  a fixed vector. This section studies the distribution of  $S = \langle \mathbf{Y} | \mathbf{m} \rangle$ . To generate  $\mathbf{Y}$ , we can first generate a multivariate Gaussian vector  $\mathbf{G} = (G_1, \dots, G_d)^\top \sim \mathcal{N}(\mathbf{0}, \mathbf{I}_d)$ , where  $\mathbf{I}_d$  is  $d \times d$  identity matrix, and set  $\mathbf{Y} = \mathbf{G} / \|\mathbf{G}\|$ . This means that  $G_i$  are i.i.d. Gaussian distributed:  $G_i \sim \mathcal{N}(0, 1)$ . Without loss of generality, using symmetry of the Euclidean norm, assume that  $\mathbf{m} = (\|\mathbf{m}\|, 0, \dots, 0)$ . This simplifies into

$$S = \langle \mathbf{Y} | \mathbf{m} \rangle = \|\mathbf{m}\| \frac{G_1}{\sqrt{\sum_{i=1}^d G_i^2}}. \quad (20)$$

Obviously,  $-\|\mathbf{m}\| \leq S \leq \|\mathbf{m}\|$  so that its cdf  $F_S(s)$  equals 0 if  $s \leq -\|\mathbf{m}\|$ , and 1 if  $s \geq \|\mathbf{m}\|$ .

For all  $s$  in the interval  $0 \leq s \leq \|\mathbf{m}\|$ ,  $\mathbb{P}(S \geq s)$  is the probability that vector  $\mathbf{G}$  belongs to the convex cone pointing in the direction  $\mathbf{m}$  and with angle  $\cos^{-1}(s/\|\mathbf{m}\|)$  since  $S/\|\mathbf{m}\|$  is the cosine of the angle between vector  $\mathbf{G}$  (or  $\mathbf{Y}$ ) and  $\mathbf{m}$ . By a symmetry argument (replacing  $\mathbf{m}$  by  $-\mathbf{m}$ ),  $\mathbb{P}(S \leq -s) = \mathbb{P}(S \geq s)$ , giving

$$F_S(-s) = 1 - F_S(s), \quad \forall 0 \leq s \leq \|\mathbf{m}\|. \quad (21)$$

It also implies that

$$\mathbb{P}(S^2 \geq s^2) = \mathbb{P}(S \geq s) + \mathbb{P}(S \leq -s) = 2(1 - F_S(s)). \quad (22)$$

Going back to  $\mathbf{G}$ , we can write

$$\begin{aligned} \mathbb{P}(S^2 \geq s^2) &= \mathbb{P}\left(\frac{G_1^2}{\sum_{i=1}^d G_i^2} \geq \tau^2\right) \\ &= \mathbb{P}\left(\frac{G_1^2}{\sum_{i=2}^d G_i^2} \geq \frac{\tau^2}{1 - \tau^2}\right), \end{aligned} \quad (23)$$

with  $\tau = s/\|\mathbf{m}\|$ . By definition, the random variable  $U = (d-1)G_1^2/\sum_{i=2}^d G_i^2$  has an F-distribution  $F(1, d-1)$ . It follows that

$$\mathbb{P}(S^2 \geq \tau^2 \|\mathbf{m}\|^2) = 1 - I_{\tau^2}(1/2, (d-1)/2), \quad (24)$$

where  $I_x(a, b)$  is the regularized incomplete beta function. In the end, for all  $s$  satisfying  $0 \leq s \leq \|\mathbf{m}\|$  we have

$$F_S(s) = \left(1 + I_{\frac{s^2}{\|\mathbf{m}\|^2}}\left(\frac{1}{2}, \frac{d-1}{2}\right)\right)/2. \quad (25)$$

By taking the derivative of this expression and accounting for symmetry, the pdf found to be:

$$f_S(s) = \frac{(1 - s^2/\|\mathbf{m}\|^2)^{\frac{d-3}{2}}}{\|\mathbf{m}\|B(1/2, (d-1)/2)}, \forall s, -\|\mathbf{m}\| \leq s \leq \|\mathbf{m}\|$$

where  $B(a, b)$  is the beta function. This implies that  $\mathbb{E}[S] = 0$  and

$$\begin{aligned} \mathbb{V}[S] &= \frac{\|\mathbf{m}\|^2}{B\left(\frac{1}{2}, \frac{d-1}{2}\right)} \int_0^1 a^2(1-a^2)^{\frac{d-3}{2}} da \\ &= \|\mathbf{m}\|^2 \frac{B\left(\frac{1}{2}, \frac{d-3}{2}\right)}{B\left(\frac{1}{2}, \frac{d-1}{2}\right)} = \frac{\|\mathbf{m}\|^2}{d}. \end{aligned}$$

When  $d \rightarrow \infty$ , using the expansion [25, Eq. (26)] of the regularized incomplete beta function in (25) yields

$$F_S(s) \approx \Phi\left(\sqrt{\frac{d-1}{\|\mathbf{m}\|^2}} \frac{2s}{1 + \sqrt{1 - s^2/\|\mathbf{m}\|^2}}\right), \quad (26)$$

which is approximately  $\Phi(\sqrt{d/\|\mathbf{m}\|^2}s)$  for small  $s$ , i.e., the cdf of a centered Gaussian r.v. with variance  $\|\mathbf{m}\|^2/d$ .

## APPENDIX B

### EXPECTED VALUE OF $\|\mathbf{m}\|^2$

We assume that the vectors  $\mathbf{x}_i$  are not related to each other so that, for  $n < d$ ,  $\mathbf{X}$  has  $n$  linearly independent columns. Then  $\mathbf{X}^+ = (\mathbf{X}^\top \mathbf{X})^{-1} \mathbf{X}^\top$  and  $\|\mathbf{m}^*\|^2 = \mathbf{1}_n^\top (\mathbf{X}^\top \mathbf{X})^{-1} \mathbf{1}_n$ . The  $n \times n$  Gram matrix  $\mathbf{X}^\top \mathbf{X}$  is real, symmetric, and positive semi-definite, and so it has an eigendecomposition  $\mathbf{U} \Lambda \mathbf{U}^\top$ , where  $\Lambda$  is a diagonal matrix with non-negative coefficients  $\{\lambda_i\}_{i=1}^n$  and  $\mathbf{U} \mathbf{U}^\top = \mathbf{U}^\top \mathbf{U} = \mathbf{I}_n$ . Moreover,  $\text{Tr}(\mathbf{X}^\top \mathbf{X}) = \sum_{i=1}^n \lambda_i = n$  because  $[\mathbf{X}^\top \mathbf{X}]_{i,i} = \langle \mathbf{x}_i | \mathbf{x}_i \rangle = 1$ , for all  $i$ .

The first construction  $\mathbf{m} = \mathbf{X} \mathbf{1}_n$  has a square norm  $\|\mathbf{m}\|^2 = \mathbf{1}_n^\top \mathbf{X}^\top \mathbf{X} \mathbf{1}_n = \mathbf{1}_n^\top \mathbf{U} \Lambda \mathbf{U}^\top \mathbf{1}_n$ . The second construction  $\mathbf{m}^* = \mathbf{X} (\mathbf{X}^\top \mathbf{X})^{-1} \mathbf{1}_n$  has a norm  $\|\mathbf{m}^*\|^2 = \mathbf{1}_n^\top (\mathbf{X}^\top \mathbf{X})^{-1} \mathbf{1}_n = \mathbf{1}_n^\top \mathbf{U} \Lambda^{-1} \mathbf{U}^\top \mathbf{1}_n$ . It is difficult to say anything more for a given  $\mathbf{X}$ . However, if we consider  $\mathbf{X}^\top \mathbf{X}$  as a random matrix, then  $\mathbb{E}[(\mathbf{X}^\top \mathbf{X})^{-1}] - (\mathbb{E}[\mathbf{X}^\top \mathbf{X}])^{-1} = \mathbb{E}[(\mathbf{X}^\top \mathbf{X})^{-1}] - \mathbf{I}_n$  is positive semi-definite [26]. This shows that  $\mathbb{E}[\|\mathbf{m}^*\|^2] \geq \mathbb{E}[\|\mathbf{m}\|^2] = n$ ; in expectation, the second construction increases the variance of the score under  $\mathcal{H}_0$ .

To make further progress, we resort to the asymptotic theory of random matrices, and especially to the Marcenko-Pastur distribution. Suppose that both  $d$  and  $n$  tend to infinity while remaining proportional:  $n = cd$  with  $c < 1$ . The matrix  $\mathbf{X}^\top \mathbf{X}$  can be thought of as an empirical covariance matrix of the  $n$  vectors which are the columns of  $\mathbf{X}$ . These vectors are i.i.d. with bounded support components. Therefore, the marginal distribution of the  $n$  eigenvalues  $\{\lambda_i\}_{i=1}^n$  of  $\mathbf{X}^\top \mathbf{X}$  asymptotically

follows the Marcenko-Pastur distribution: for all  $\lambda$  such that  $(1 - \sqrt{c})^2 \leq \lambda \leq (1 + \sqrt{c})^2$ ,

$$f_{\text{MP}}(\lambda) = \frac{\sqrt{(\lambda - (1 - \sqrt{c})^2)((1 + \sqrt{c})^2 - \lambda)}}{2c\pi\lambda}. \quad (27)$$

Moreover, for any function  $\psi$  bounded over the interval  $[(1 - \sqrt{c})^2, (1 + \sqrt{c})^2]$ :

$$\frac{1}{n} \sum_{i=1}^n \psi(\lambda_i) - \int \psi(\lambda) f_{\text{MP}}(\lambda) d\lambda \rightarrow 0. \quad (28)$$

Using the eigendecomposition,  $\mathbf{X}^\top \mathbf{X} = \mathbf{U} \Lambda \mathbf{U}^\top$ , we get  $(\mathbf{X}^\top \mathbf{X})^{-1} = \mathbf{U} \Lambda^{-1} \mathbf{U}^\top$ , where the columns of  $\mathbf{U}$  are the random eigenvectors. Then, asymptotically as  $d \rightarrow \infty$ :

$$n^{-1} \mathbb{E}[\mathbf{1}_n^\top (\mathbf{X}^\top \mathbf{X})^{-1} \mathbf{1}_n] - \int \lambda^{-1} f_{\text{MP}}(\lambda) d\lambda \rightarrow 0. \quad (29)$$

This shows that  $\mathbb{E}[\|\mathbf{m}^*\|^2]/n$  converges to  $\frac{1}{1-c}$  asymptotically (the integral is the Stieljes transform of the Marcenko-Pastur distribution evaluated at  $z = 0$ ), whereas  $\mathbb{E}[\|\mathbf{m}\|^2]/n$  converges to 1. In expectation,  $\mathbf{m}^*$  has a higher variance, but only by a factor of  $1/(1-c)$  which remains asymptotically small if  $c = n/d$  is small.

## ACKNOWLEDGMENTS

This work was supported by ERC grant VIAMASS no. 336054.

## REFERENCES

- [1] R. Weber, H.-J. Schek, and S. Blott, "A quantitative analysis and performance study for similarity-search methods in high-dimensional spaces," in *Proceedings of the International Conference on Very Large DataBases*, 1998, pp. 194–205.
- [2] M. Muja and D. G. Lowe, "Scalable nearest neighbor algorithms for high dimensional data," *IEEE Trans. PAMI*, vol. 36, 2014.
- [3] M. S. Charikar, "Similarity estimation techniques from rounding algorithms," in *STOC*, May 2002, pp. 380–388.
- [4] R. Arandjelović and A. Zisserman, "Extremely low bit-rate nearest neighbor search using a set compression tree," *IEEE Transactions on Pattern Analysis and Machine Intelligence*, 2014.
- [5] Y. Weiss, A. Torralba, and R. Fergus, "Spectral hashing," in *NIPS*, December 2009.
- [6] W. Dong, M. Charikar, and K. Li, "Asymmetric distance estimation with sketches for similarity search in high-dimensional spaces," in *SIGIR*, July 2008, pp. 123–130.
- [7] H. Jégou, M. Douze, and C. Schmid, "Product quantization for nearest neighbor search," *IEEE Trans. PAMI*, vol. 33, no. 1, pp. 117–128, January 2011.
- [8] A. Babenko and V. Lempitsky, "The inverted multi-index," in *CVPR*, June 2012.
- [9] F. Perronnin and C. R. Dance, "Fisher kernels on visual vocabularies for image categorization," in *CVPR*, June 2007.
- [10] G. Csurka, C. Dance, L. Fan, J. Willamowski, and C. Bray, "Visual categorization with bags of keypoints," in *ECCV Workshop Statistical Learning in Computer Vision*, 2004.
- [11] J. Sivic and A. Zisserman, "Video Google: A text retrieval approach to object matching in videos," in *ICCV*, October 2003, pp. 1470–1477.
- [12] H. Jégou, M. Douze, C. Schmid, and P. Pérez, "Aggregating local descriptors into a compact image representation," in *CVPR*, June 2010.
- [13] L. Bo and C. Sminchisescu, "Efficient match kernels between sets of features for visual recognition," in *NIPS*, 2009.
- [14] H. Jégou and A. Zisserman, "Triangulation embedding and democratic kernels for image search," in *CVPR*, June 2014.
- [15] N. Murray and F. Perronnin, "Generalized max-pooling," in *CVPR*, June 2014.
- [16] J. Philbin, O. Chum, M. Isard, J. Sivic, and A. Zisserman, "Object retrieval with large vocabularies and fast spatial matching," in *CVPR*, June 2007.

- [17] H. Jégou, M. Douze, and C. Schmid, "Hamming embedding and weak geometric consistency for large scale image search," in *ECCV*, October 2008.
- [18] D. Nistér and H. Stewénius, "Scalable recognition with a vocabulary tree," in *CVPR*, June 2006, pp. 2161–2168.
- [19] C. R. Rao and S. K. Mitra, *Generalized inverse of matrices and its applications*, 1971, vol. 7.
- [20] C. M. Bishop *et al.*, *Pattern recognition and machine learning*. Springer New York, 2006, vol. 1.
- [21] A. Babenko, A. Slesarev, A. Chigorin, and V. Lempitsky, "Neural codes for image retrieval," in *ECCV*, 2014.
- [22] I. S. Dhillon and D. S. Modha, "Concept decompositions for large sparse text data using clustering," *Machine learning*, vol. 42, no. 1-2, pp. 143–175, 2001.
- [23] A. Gordo and F. Perronnin, "Asymmetric distances for binary embeddings," in *CVPR*, 2011.
- [24] M. Jain, H. Jégou, and P. Gros, "Asymmetric hamming embedding," in *ACM Multimedia*, October 2011.
- [25] A. R. DiDonato and M. P. Jarnagin, "A method for computing the incomplete beta function ratio," Computation and Analysis laboratory, U.S. Naval Weapons Laboratory, Dahlgren, VI, USA, Tech. Rep. No. 1949, Oct. 1966.
- [26] T. Groves and T. Rothenberg, "A note on the expected value of an inverse matrix," *Biometrika*, vol. 56, no. 3, pp. 690–691, Dec. 1969.